

New H α Flux Measurements in Nearby Dwarf Galaxies

S. S. Kaisin^{1,*} and I. D. Karachentsev^{1,**}

¹*Special Astrophysical Observatory, Russian Academy of Sciences, Russia*
(Received September 2, 2014; Revised September 8, 2014)

We present the emission H α line images for 40 galaxies of the Local Volume based on the observations at the 6-meter BTA telescope. Among them there are eight satellites of the Milky Way and Andromeda (M31) as well as two companions to M51. The measured H α fluxes of the galaxies are used to determine their integral (SFR) and specific (sSFR) star formation rates. The values of log sSFR for the observed galaxies lie in the range of $(-9, -14)$ [yr⁻¹]. A comparison of SFR estimates derived from the H α flux and from the ultraviolet FUV flux yields evidence that two blue compact galaxies MRK 475 and LV J1213+2957 turn out to be at a sharp peak of their star-burst activity.

1. INTRODUCTION

This work is a continuation of papers [1–8] determining the rate of star formation in the galaxies of the Local Volume measuring their integral flux in the emission H α Balmer line. Our program provides measurements of the H α flux at the 6-m telescope of the Special Astrophysical Observatory for all galaxies of the northern sky with distances within $D \leq 11$ Mpc which were not covered by observations at other telescopes.

The latest version of the Updated Nearby Galaxy Catalog (UNGC) [9] contains 869 objects with distance estimates within $D < 11$ Mpc or with the line-of-sight velocities relative to the centroid of the Local Group $V_{LG} < 600$ km s⁻¹. During 2014 this sample has been supplemented with forty new galaxies included in the database [10], which is available at <http://www.sao.ru/lv/lvgdb>. In total the current database of the Local Volume contains H α flux measurements for approximately 550 galax-

ies, where the fluxes for more than 350 galaxies were measured with the 6-m BTA telescope.

The H α line images of nearby galaxies make it possible to study the distribution of the centers of star formation that formed in the galaxies over the past 10–30 myr. A comparison of the H α -emission map of the galaxy with the distribution of atomic and molecular hydrogen in it allows a detailed study of the conditions under which a transformation of the gas component in the galaxy into stars takes place.

Of particular interest in this respect are the dwarf galaxies with their shallow gravitational wells, owing to which dwarf systems easily lose their gas component under the effect of the supernova burst or during the motion through the halo of hot gas around a massive neighboring galaxy. Being sensitive to the environment, dwarf galaxies are often used as “test particles” for the analysis of the dynamical evolution of both galaxy clusters and the population of the general field.

Below we present the H α images, the H α flux values, and the star formation rate (SFR) estimates for forty galaxies of the Local Volume and one object, KKR 9, which turned out to be an

* Electronic address: skai@sao.ru

** Electronic address: ikar@sao.ru

interstellar cirrus. All but two galaxies are dwarf systems of late or early types.

2. OBSERVATIONS AND DATA REDUCTION

The images in the $H\alpha$ line and in the neighboring continuum were obtained in the period from February to December 2013. The observations were carried out at the prime focus of the BTA with the SCORPIO focal reducer [11] equipped with a 2048×2048 pixel CCD, in the 2×2 binning mode. The optical system provided a field of view of $6'.1 \times 6'.1$ at the scale of $0''.185$ per pixel.

The images in the $H\alpha + [NII]$ lines were obtained using a narrowband interference filter with the effective wavelength of 6555 \AA and the full width at half maximum of 75 \AA . The images in the continuum were taken with midband filters SED 607 ($\lambda_e = 6063 \text{ \AA}$, $\Delta\lambda = 167 \text{ \AA}$) and SED 707 ($\lambda_e = 7036 \text{ \AA}$, $\Delta\lambda = 207 \text{ \AA}$). Owing to a small range of line-of-sight velocities of the galaxies, all the objects were observed with one and the same filter set. The typical total exposure in the $H\alpha$ line was 1200 s.

For processing the observed data, standard procedures were used: bias subtraction, flat-field correction, removing cosmic ray hits, sky background subtraction. The images in the continuum were normalized to the $H\alpha$ images using the non-overexposed stars and were then subtracted. Integral $H\alpha$ fluxes of galaxies were measured from the $H\alpha$ images with subtracted continuum. To calibrate the flux, the images of the spectrophotometric standard stars [12] were used which were observed at the same night with the objects. A typical $H\alpha$ flux logarithm measurement error in our images is ± 0.1 [8].

3. RESULTS OF OBSERVATIONS

The mosaic image of forty-one observed objects is given in the Appendix, where the left-hand-side images correspond to the total exposure in the $H\alpha$ line and the continuum, and the right-hand-side images are the $H\alpha$ line images after subtracting the continuum. The image scale and their “north-east” orientation are marked at the bottom of the right-hand-side images. After the continuum subtraction many images reveal residual “caverns” caused by the saturation of stellar images in high-brightness stars. Another reason may be an abnormal color index of stars or different image quality in the $H\alpha$ filter and in the continuum. In fact, it is the presence of such residual components that determines the accuracy limit when detecting the $H\alpha$ flux of the galaxy, especially if it has a low surface brightness and large size or is located in a dense stellar field at a low galactic latitude.

Following [13], we determine the integral star formation rate in the galaxy using the relation

$$\log \text{SFR} = \log F_c(H\alpha) + 2 \log D + 8.98,$$

where $F_c(H\alpha)$ is the integral flux in the $H\alpha$ line in the units of $\text{erg cm}^{-2} \text{ s}^{-1}$, corrected for the absorption of light in the Galaxy according to [14], D is the distance in Mpc, and SFR is expressed in M_\odot/year . We have ignored the internal absorption of light in the galaxy as well as the contribution of the emission [NII] doublet, since both effects are negligibly small for dwarf galaxies [15, 16].

The table contains the main data on the observed galaxies. Its columns show: (1) the name of the galaxy, (2) equatorial coordinates for the epoch (J2000.0), (3) integral apparent B magnitude from the UNGC catalog [9], (4) morphological type by the de Vaucouleurs scale, (5) distance to the galaxy in Mpc according to the

UNGC catalog data [9], (6) logarithm of the observed galaxy flux in the $H\alpha$ line in the units of $\text{erg cm}^{-2} \text{s}^{-1}$, (7) logarithm of the integral star formation rate in M_{\odot}/year , (8) specific star formation rate $\text{sSFR} = \text{SFR}/M^*$, where M^* is the stellar mass of the galaxy from catalog [9], determined from the K -band luminosity. The last column shows for comparison the integral starburst rate of the galaxy [16]

$$\log \text{SFR} = \log F_c(\text{FUV}) + 2 \log D - 6.78$$

determined by its flux in the far ultraviolet ($\lambda_e = 1539 \text{ \AA}$, $\text{FWHM} = 269 \text{ \AA}$), measured by the GALEX satellite [17], corrected for the extinction of light in the Galaxy.

4. FEATURES OF SOME OBSERVED GALAXIES

With the exception of two late-type spiral galaxies MCG +09-16-010 (Sm) and UGC 5047 (Sdm), all the remaining observed objects are dwarf galaxies of late (Ir, Im, BCD) or early (dSph) type. Note the most remarkable among them.

AndXXXII = *Cas III*, *AndXXXIII* = *Perseus I*, *AndXXXI* = *Lacerta I*. These three dSph companions of M31 were recently detected within the 3π Pan-STARRS1-survey [18, 19]. All three objects do not reveal any signs of emission. The table lists for them only the upper limits of the integral $H\alpha$ flux. We should, however, note that the angular diameters of these nearby dwarf systems are quite large: $13'0$ (Cas III), $3'4$ (Pers I), and $8'4$ (Lac I), and in two cases they exceed the field of view of our detector.

PAndAS-48. A distant globular cluster at the far periphery of M31 [20].

DGSAT-I. A dwarf spheroidal galaxy in the neighborhood of M31 [21]. Its radial velocity

is not known, and the distance, measured as 8.0 Mpc, is very unreliable.

Segue 2, *UMa I*, *CVn I*, *Segue 3*. Four dShp companions of the Milky Way, detected in [22–25] respectively. The table lists for them only the upper value of the $H\alpha$ flux. It should be borne in mind that the angular dimensions of UMa I ($18'0$) and CVn I ($14'3$) significantly exceed the field of view of the SCORPIO focal reducer.

NGC 1400. An elliptical galaxy in the Eridanus group at the distance of 24.9 Mpc [26]. It formally makes it into the sample of the Local Volume by its line-of-sight velocity $V_{\text{LG}} = 496 \text{ km s}^{-1}$. Its peculiar line-of-sight velocity relative to the Eridanus group is -1320 km s^{-1} . The presence of $H\alpha$ emission in its central part is not typical for the E galaxies in the groups, but the GALEX data [17] indicate active star formation in the center of NGC 1400.

NGC 1592. A knotty dIr galaxy with a high specific star formation rate.

HIPASS J0705–20. This radio source with the radial velocity $V_{\text{LG}} = 528 \text{ km s}^{-1}$ [27] has no optical identification, although the magnitude of the Galactic extinction in its direction is not too large, $A_B = 2^m71$ [14]. The $H\alpha$ image we have obtained reveals one diffuse spot with the coordinates $070546.95\text{--}205932.6$ and two point knots with the coordinates $070543.31\text{--}205935.1$ and $070545.87\text{--}205837.7$, which can belong to an irregular galaxy of low surface brightness. Radial velocity measurement for these objects will be a crucial test for the accuracy of radio source identification.

Leo P. A very nearby dIr galaxy with radial velocity of $V_{\text{LG}} = 135 \text{ km s}^{-1}$ [28]. The main $H\alpha$ flux comes from a compact HII region near the center of the object.

LVJ1213+2957. A compact blue HII region detected in the SDSS [29]. Having a

Parameters of the observed galaxies

Name	RA, Dec	B_t	T	D	$\log F$	$\log \text{SFR}$	$\log \text{sSFR}$	$\log \text{SFR}_{\text{FUV}}$
And XXXII = C as III	003559.4+513335	13.7	-3	0.78	< -15.28	< -6.35	< -13.92	-
P And AS-48	005928.2+312910	20.5	-3	0.82	< -15.17	< -6.30	< -10.99	< -6.37
DGSAT-I	011736.2+333134	18.2	-2	8.0	< -15.23	< -4.39	< -11.95	-3.86
Segue 2	021916.0+201031	16.2	-3	0.03	< -15.37	< -9.14	< -13.02	-7.92
And XXXIII = Pers I	030123.6+405918	15.5	-2	0.79	< -15.28	< -6.38	< -13.19	-
NGC 1400	033930.8-184117	11.9	-3	24.9	-12.49	-0.66	-11.65	-1.21
NGC 1592	042940.8-272431	14.5	10	9.1	-12.21	-1.28	-9.46	-0.93
ESO 489-056	062617.0-261556	15.7	10	4.99	-13.19	-2.75	-10.24	-
HIPASS J0705-20	070545.0-205930	-	10	7.2	-14.46	-3.18	-	-
LV J0737+4724	073728.5+472433	18.1	10	15.7	-14.30	-2.83	-10.44	-2.48
LV J0812+4836	081239.5+483645	17.1	9	12.4	-13.92	-2.70	-10.40	-2.46
KUG 0821+3201	082505.0+320103	16.8	10	8.2	-13.61	-2.77	-10.21	-
AGC 182595	085112.1+275248	17.2	9	9.04	-13.78	-2.85	-10.22	-2.87
LV J0913+1937	091339.0+193708	17.4	10	4.4	-13.82	-3.51	-10.18	-3.36
AGC 198508	092257.0+245648	17.8	10	10.4	-13.52	-2.47	-9.71	-
MCG +09-16-010	092317.0+515822	16.2	8	7.4	-13.43	-2.70	-10.34	-2.42
UGC 5047	092849.6+513338	16.0	7	19.7	-13.82	-2.22	-10.94	-
KUG 0937+4800	094019.6+474638	17.0	9	7.9	-13.83	-3.04	-10.32	-2.71
LV J1000+5022	100025.5+502245	17.1	9	8.0	-13.68	-2.89	-10.13	-
LV J1000+3032	100036.5+303210	18.1	10	7.1	-14.58	-3.88	-10.65	-3.39
LV 1021+0054	102138.9+005400	17.5	10	6.8	-13.71	-3.02	-10.03	-2.78
Leo P	102145.1+180517	17.2	10	2.0	-13.69	-4.08	-10.11	-
LV J1030+0607	103044.3+060738	16.8	10	7.8	-14.01	-3.22	-10.59	-2.73
AGC 731457	103155.8+280133	16.8	10	11.12	-13.73	-2.63	-10.31	-2.27
UMa I	103452.8+515512	15.3	-3	0.10	< -15.28	< -8.28	< -13.16	< -8.36
KUG 1033+366B	103617.6+362531	17.0	9	8.1	-13.60	-2.78	-10.09	-2.74
LV J1052+3628	105205.5+362836	17.9	10	9.2	-14.40	-3.48	-10.53	-2.93
LV J1213+2957	121348.4+295732	17.4	10	2.7	-13.38	-3.53	-9.72	-3.92
KKH 78	121744.5+332043	17.7	10	4.7	< -15.30	< -4.96	< -11.51	-4.95
DDO 120	122115.0+454841	13.6	9	7.1	-15.15	-4.46	-13.17	-1.96
GR 34	122207.6+154757	16.0	10	9.29	-14.39	-3.45	-11.31	-2.82
KDG 215	125540.5+191233	16.9	10	4.83	-15.17	-4.80	-11.70	-3.33
CVn I	132803.5+333321	13.9	-3	0.22	< -15.32	< -7.62	< -13.73	< -7.67
UGCA 361	133236.2+494949	16.7	-1	8.0	< -15.26	< -4.47	< -12.57	-4.12
MCG +08-25-028	133644.8+443557	15.9	10	7.7	-13.30	-2.52	-10.23	-2.54
KKR 9	142705.0+224125	-	-	-	< -15.24	< -5.51	-	-
MRK 475	143905.4+364822	16.4	9	9.2	-12.41	-1.50	-9.14	-2.24
UGC 9660	150109.3+444153	14.4	9	7.4	-12.62	-1.88	-10.25	-1.81
UGC 9992	154147.8+671515	15.4	10	7.3	-13.04	-2.30	-10.19	-2.02
Segue 3	212131.0+190702	15.9	-3	0.02	< -15.37	< -9.86	< -13.06	< -9.67
And XXXI = Lac I	225816.3+411728	14.0	-3	0.76	< -15.28	< -6.42	< -13.77	-

small radial velocity, $V_{\text{LG}} = 196 \text{ km s}^{-1}$, it is probably part of the group of five galaxies around NGC 4150 at a distance of approximately 16 Mpc, which has a collective peculiar velocity of about -700 km s^{-1} [30].

KKH 78. An irregular galaxy of low surface brightness with no signs of $\text{H}\alpha$ emission, a probable companion of the NGC 4395 galaxy.

DDO 120 = UGC 7408. A bluish Magellanic-type irregular galaxy with no H II regions. A very weak diffuse $\text{H}\alpha$ emission gives the 300 times lower star formation rate than that from the FUV flux measured by the GALEX.

GR 34 = VCC 530, KDG 215. Two dIr galaxies in front of the Virgo Cluster, the distances to which were measured in [31]. KDG 215 shows

only a very weak diffuse emission.

UGCA 361, MCG +08-25-028. These are the dSph and dIr companions of M 51.

KKR 9. This object proved to be not a dwarf galaxy but a fragment of an interstellar cirrus.

MRK 475. A blue compact galaxy of high surface brightness. One of the most active objects of the Local Volume. Judging by the specific star formation rate $\log(\text{sSFR}) = -9.14 \text{ [yr}^{-1}\text{]}$, this dwarf system is at the peak of its starburst activity.

UGC 9660, UGC 9992. Both dwarf galaxies have vigorous centers of star formation. Their distances, determined by the Tully–Fisher relation [32], 7.4 Mpc and 7.3 Mpc, almost coincide with the distance to M 101 (7.38 Mpc). Both galaxies can be associated with the group M 101, although their radial velocities $+745 \text{ km s}^{-1}$ and $+638 \text{ km s}^{-1}$ are significantly larger than that of M 101 ($+378 \text{ km s}^{-1}$).

5. DISCUSSION AND CONCLUSIONS

As we can see from the last column of the table, thirty out of forty galaxies we have observed have independent SFR estimates from the ultraviolet flux measured by the GALEX satellite. A fairly clear correlation is noticeable between the SFR estimates by the $\text{H}\alpha$ flux and FUV flux, which is smeared in weak fluxes. For twenty galaxies with the $\log \text{SFR}(\text{H}\alpha) > -4.0$ estimates, the average difference between the values is

$$\langle \log \text{SFR}(\text{H}\alpha) - \log \text{SFR}(\text{FUV}) \rangle = -0.16 \pm 0.08$$

with a standard deviation of 0.35. This difference is somewhat larger than the typical measurement error of the $\text{H}\alpha$ flux (± 0.10) logarithm and the FUV flux logarithm (± 0.04).

The reasons of the differences between the SFR estimates based on the $\text{H}\alpha$ line emission

and the ultraviolet flux of the galaxies were discussed by many authors, in particular, in [16] and [32]. As it was noted in [33], the star formation rate by the $\text{H}\alpha$ flux relative to the FUV flux for the dwarf galaxies of very low luminosity may be underestimated by ten or more times. The empirical mutual normalization of $\text{SFR}(\text{H}\alpha) \simeq \text{SFR}(\text{FUV})$ was made by the spiral galaxies. It is not well suited to the dwarf systems, where the initial stellar mass function at its bright end may be substantially different than that of the spiral galaxies. It should also be remembered that the SFR estimation based on the $\text{H}\alpha$ flux corresponds to the characteristic time of about 10^7 yr , whereas the SFR determined by the FUV flux covers the range of approximately 10^8 yr . In the presence of star formation bursts, especially noticeable in dwarf galaxies, the $\text{SFR}(\text{H}\alpha)/\text{SFR}(\text{FUV})$ ratio indicates the phase of activity in which the galaxy dwells. For example, blue compact galaxies MRK 475 and LV J1213+2957 are obviously observed at the peak of their starburst activity. On the other hand, dwarf galaxies DDO 120 and KDG 215 with bluish but aged stellar population are at the stage of long-term relaxation after the activity peaks. Therefore, the SFR estimate ratio from the $\text{H}\alpha$ and FUV fluxes can be a useful indicator of the flare activity phase of a dwarf galaxy.

As noted in [34, 35], specific star formation rate $\log \text{sSFR} = \log(\text{SFR}/M^*)$ of the galaxies in the present epoch has an upper limit expressed as $-9.4 \text{ [yr}^{-1}\text{]}$. Not less than 98–99% of all galaxies are subject to this restriction. It obviously means that a too vigorous star formation leads

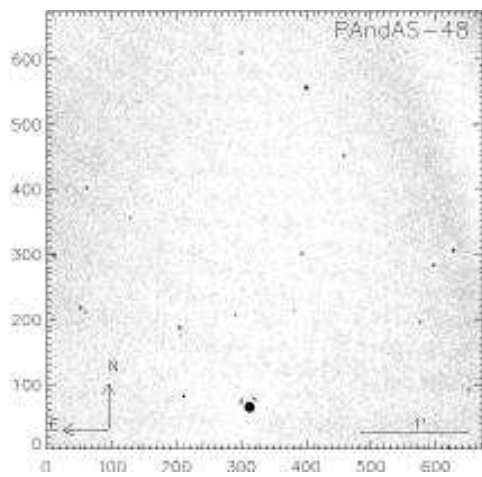
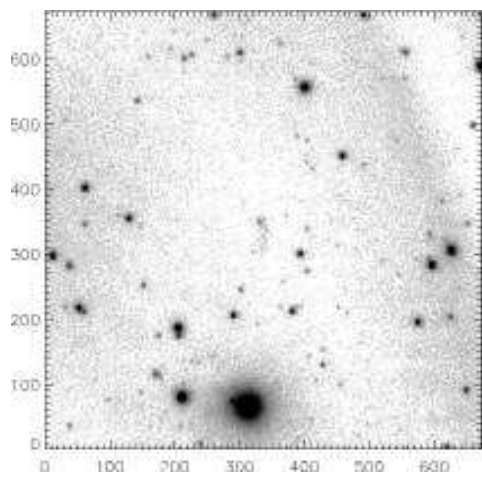
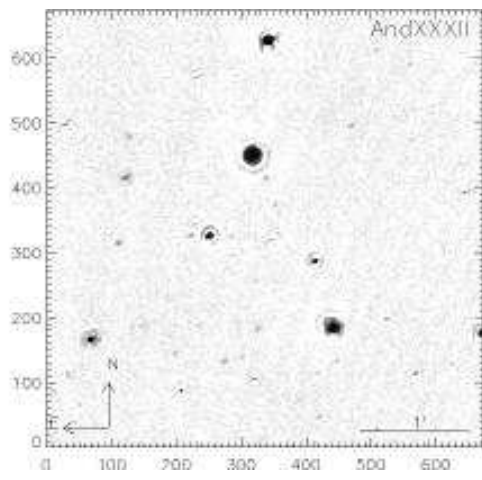
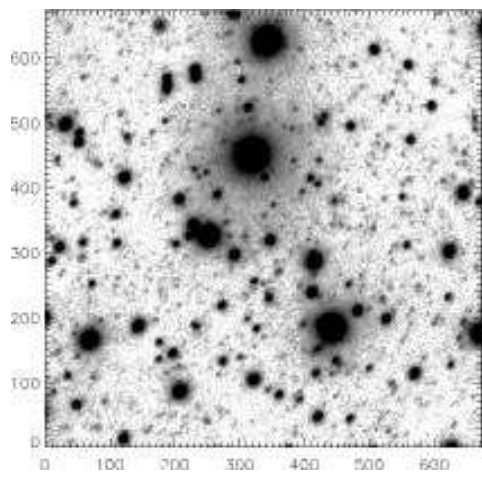
to the depletion of gas reserves in the galaxy. Among the objects of the table there is only one galaxy, MRK 475 with $\log s\text{SFR} = -9.14 \text{ [yr}^{-1}\text{]}$, which exceeds the specified limit. It should be noted, however, that the error in the determining the stellar mass in blue compact galaxies is quite large—about 50%, and this Markarian galaxy may actually not be violating the general pattern.

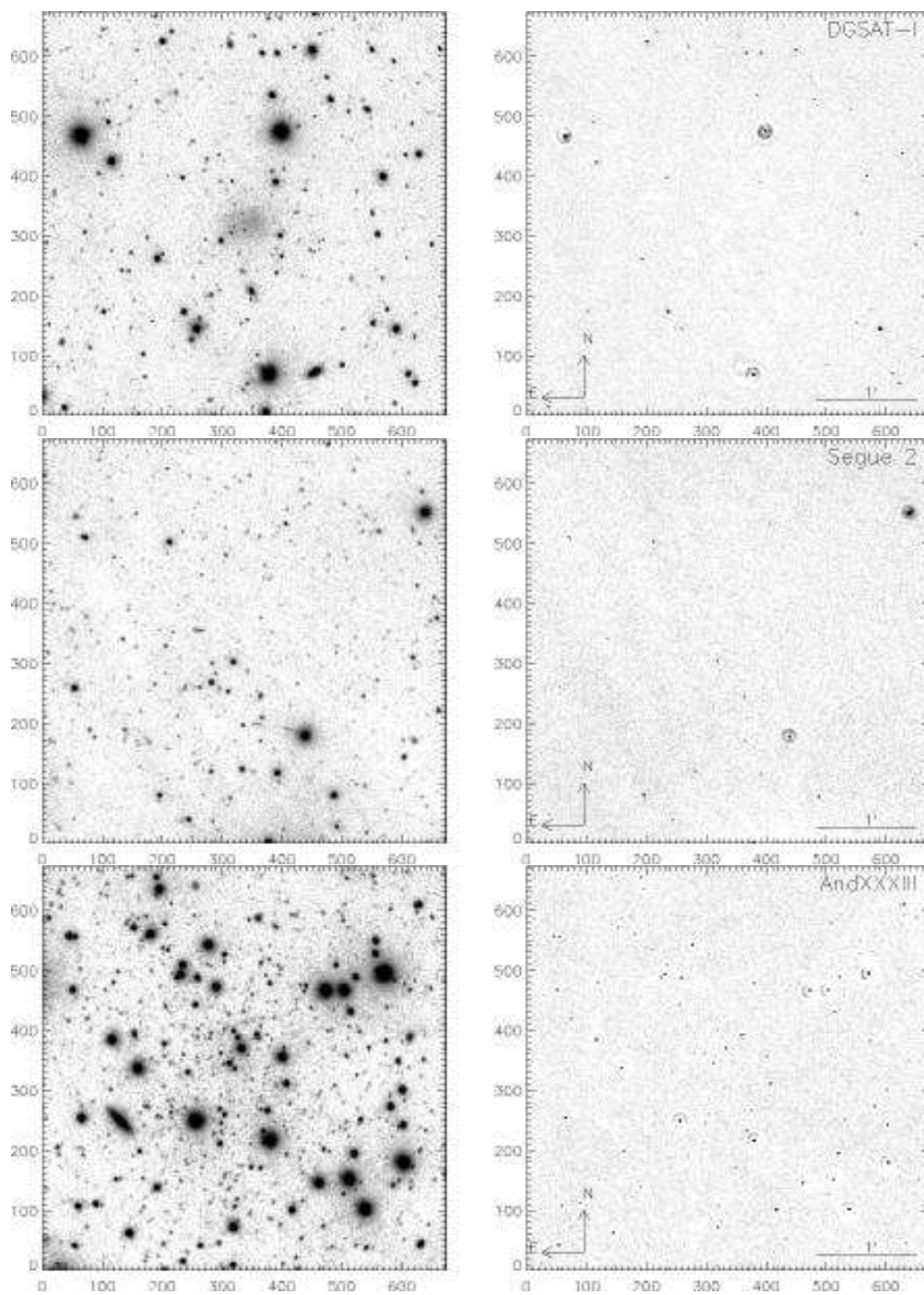
Observations at the 6-meter BTA telescope were carried out with the financial support of the Ministry of Education and Science of the Russian Federation (state contracts No. 14.518.11.7070, 16.518.11.7073).

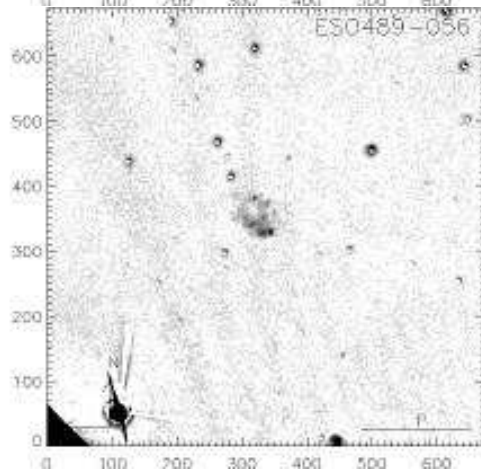
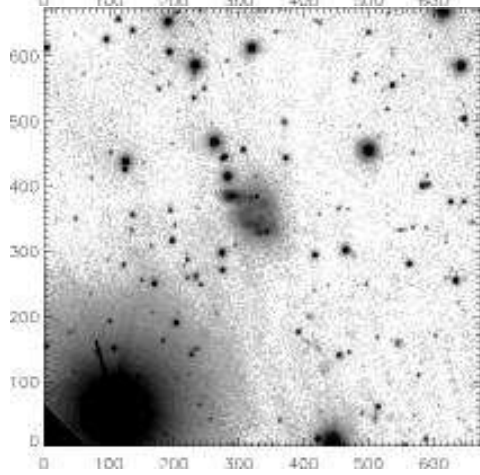
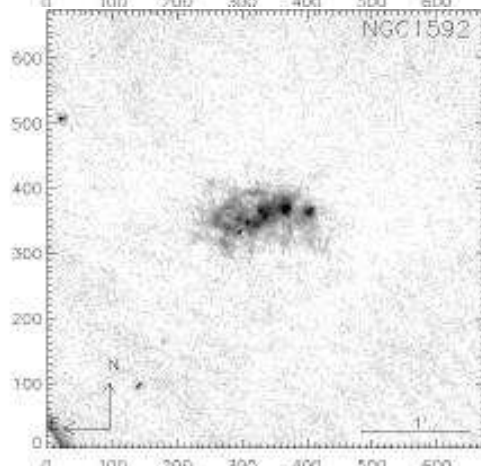
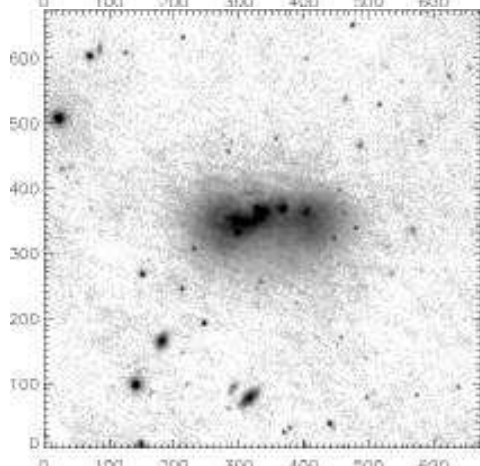
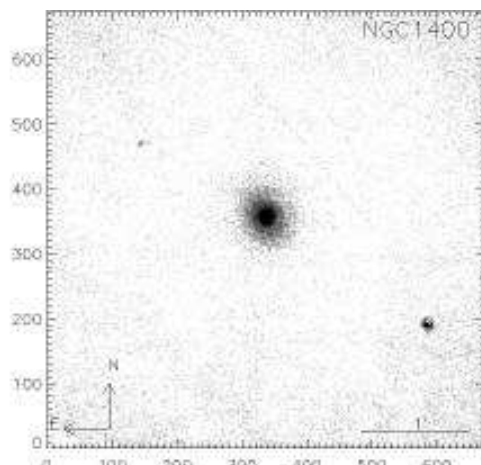
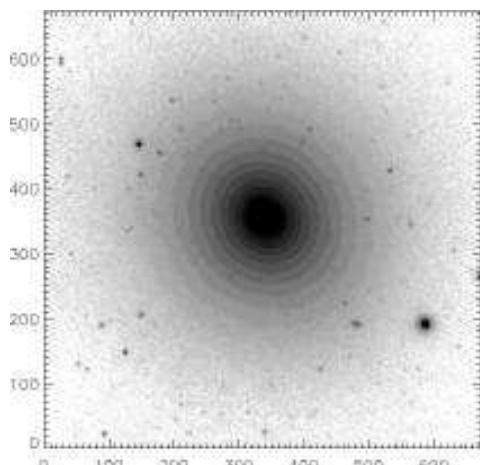
ACKNOWLEDGMENTS

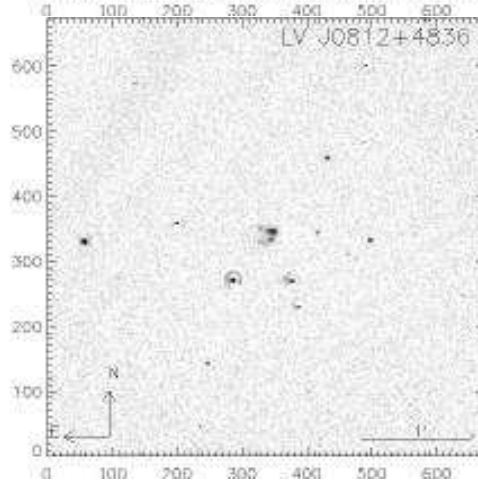
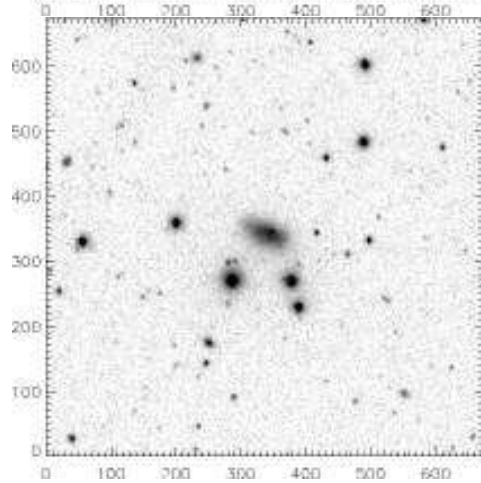
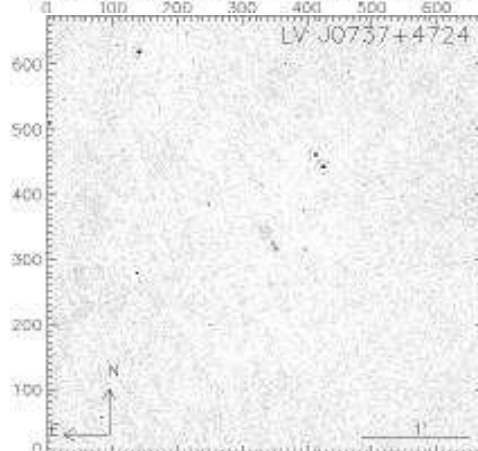
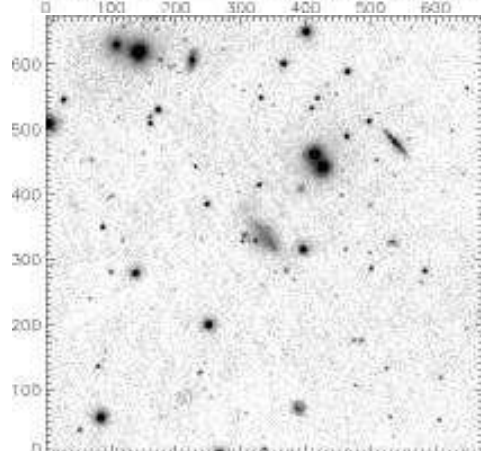
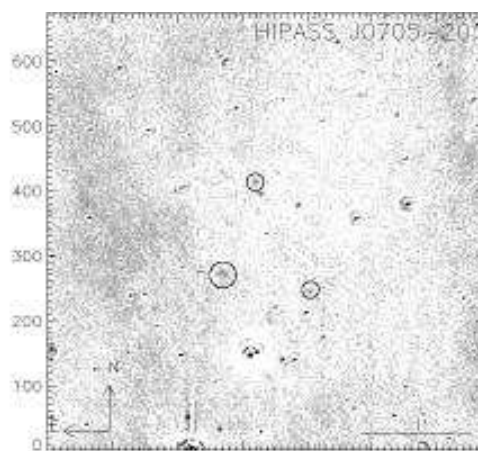
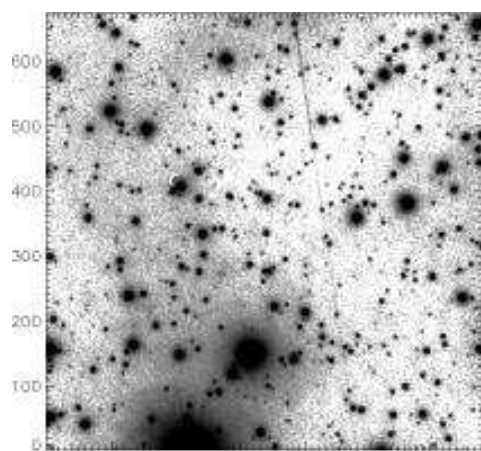
This work was supported by the RFBR grants 13-02-92960-Ind-f and 13-02-00780. The obser-

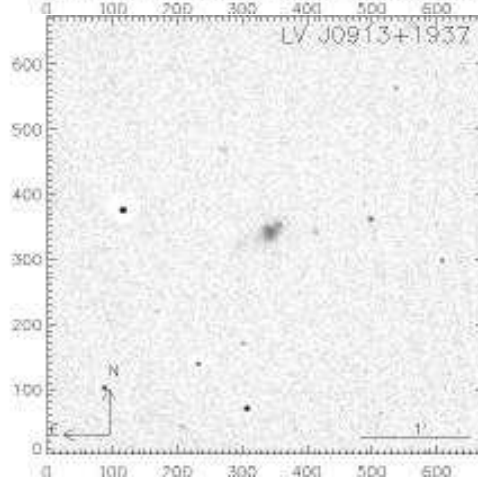
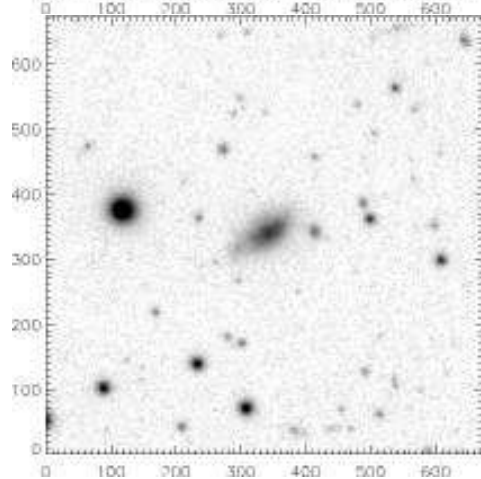
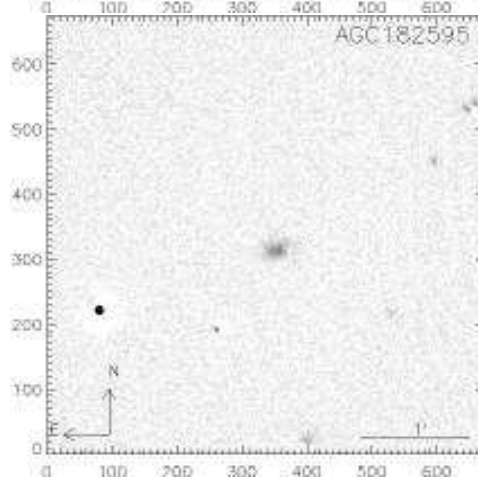
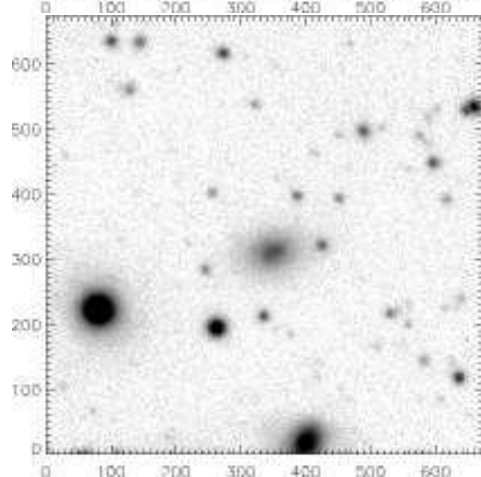
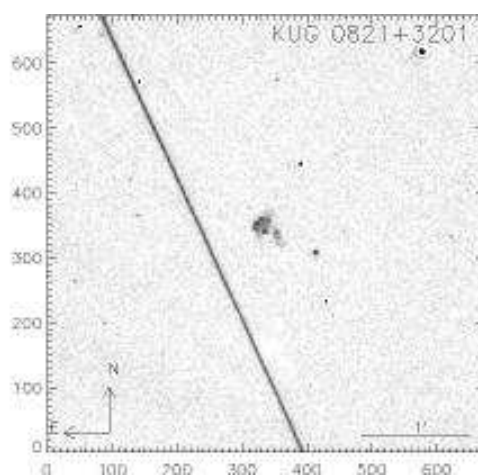
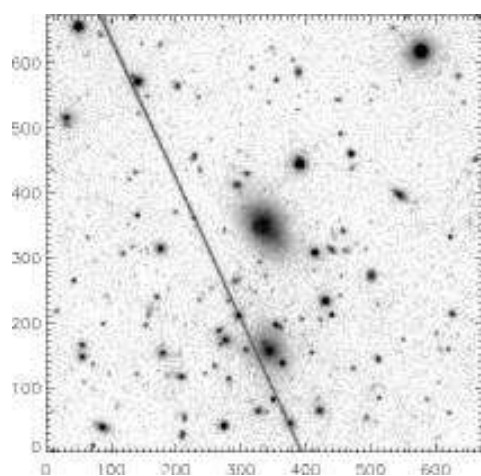
APPENDIX

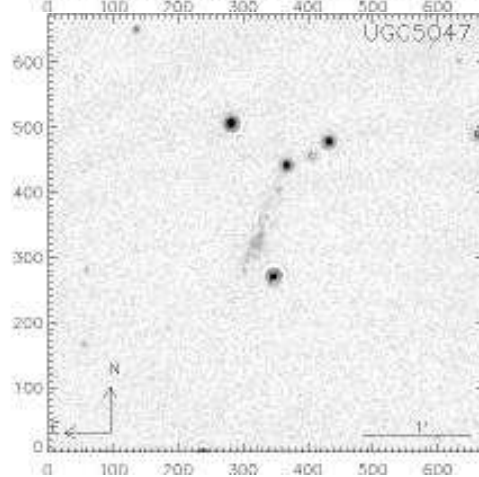
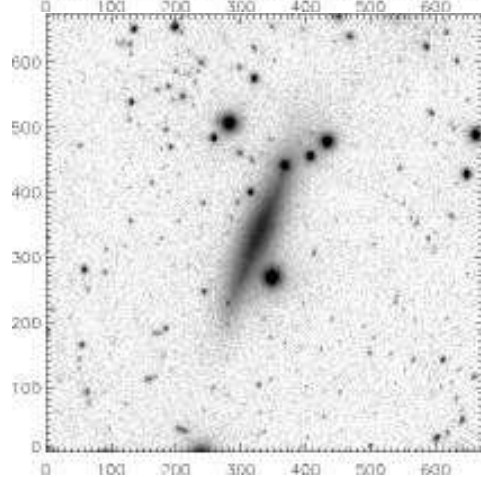
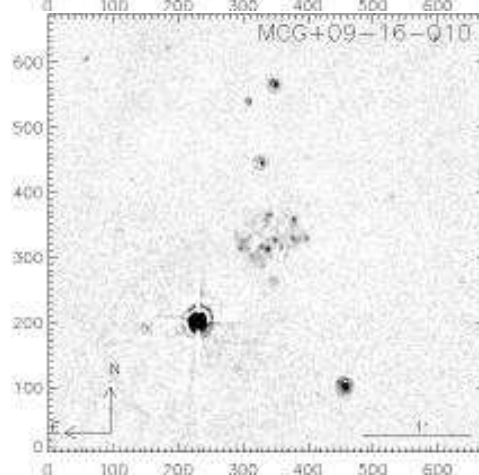
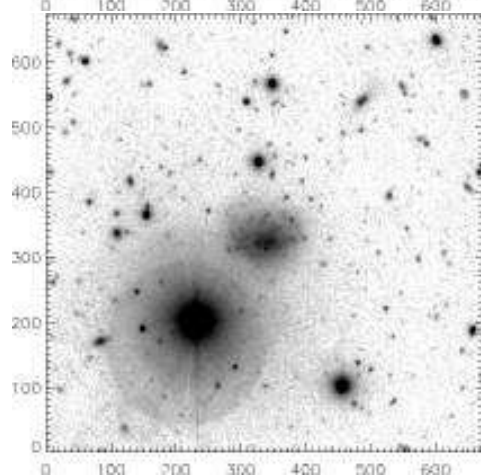
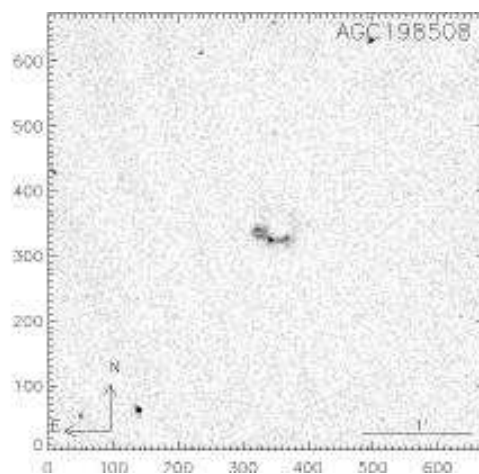
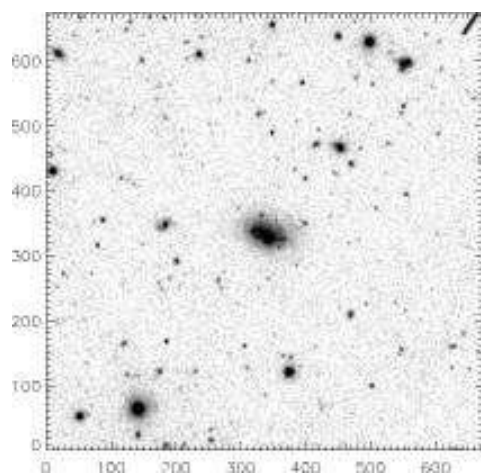


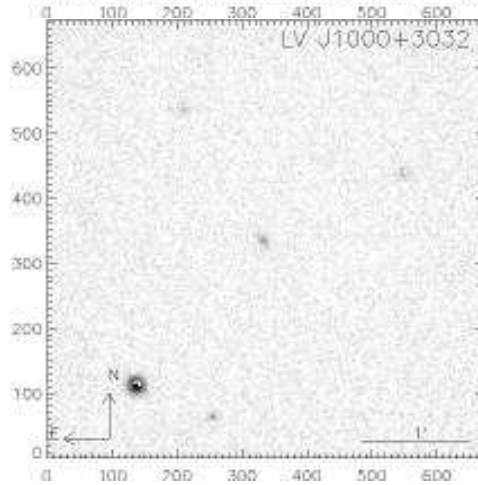
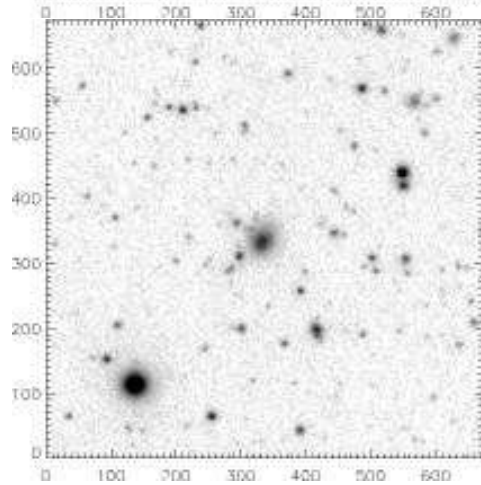
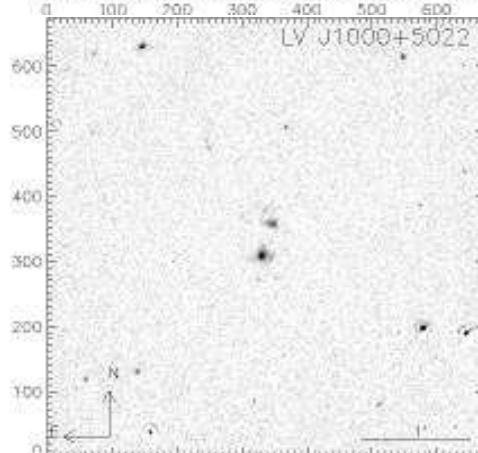
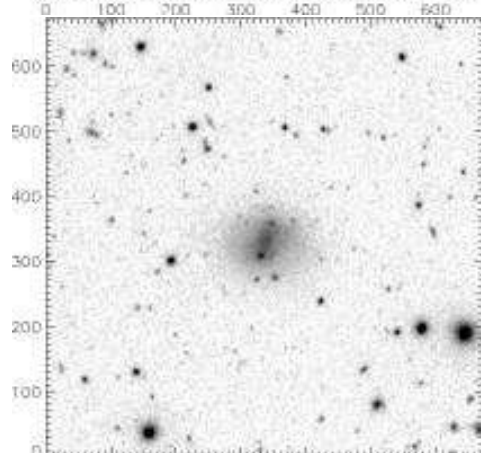
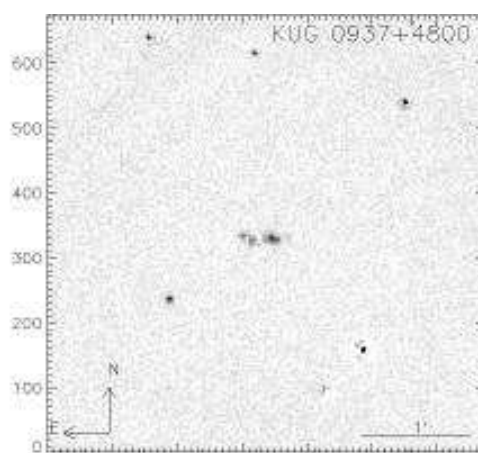
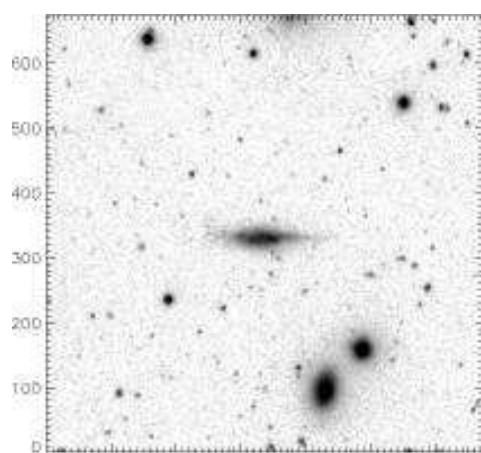


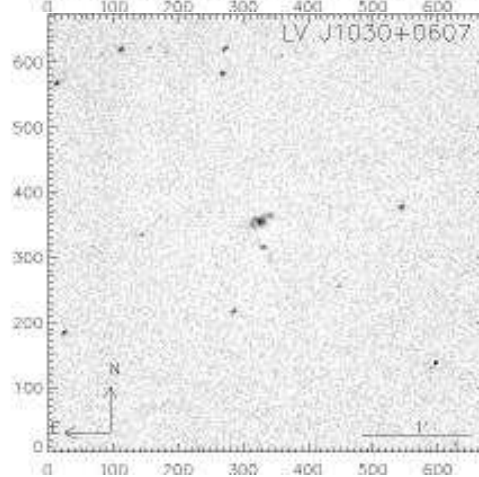
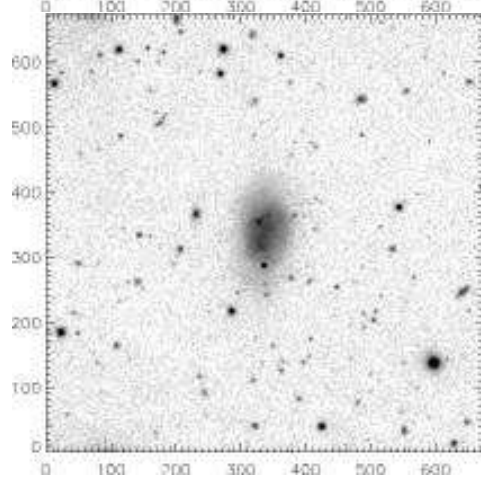
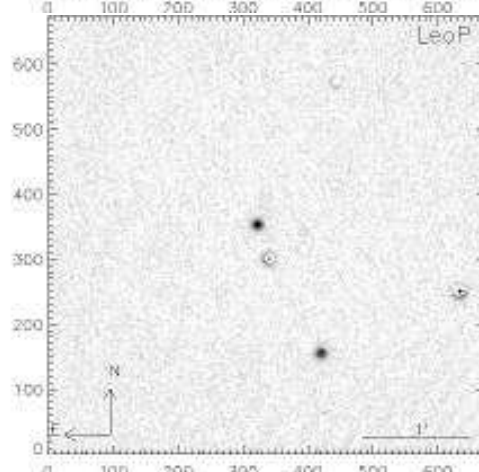
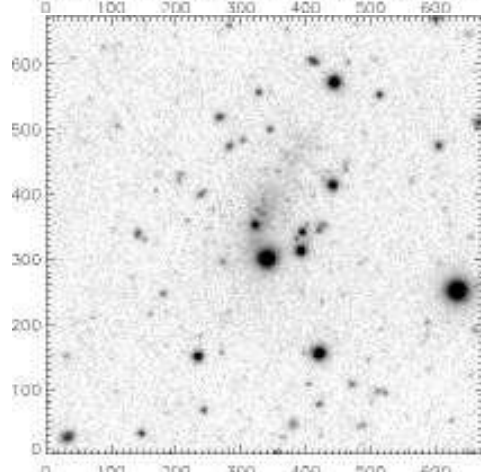
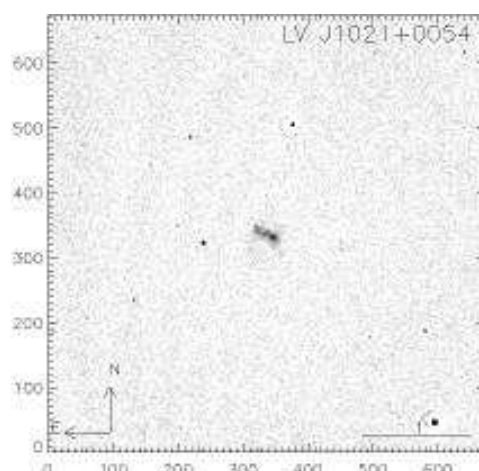
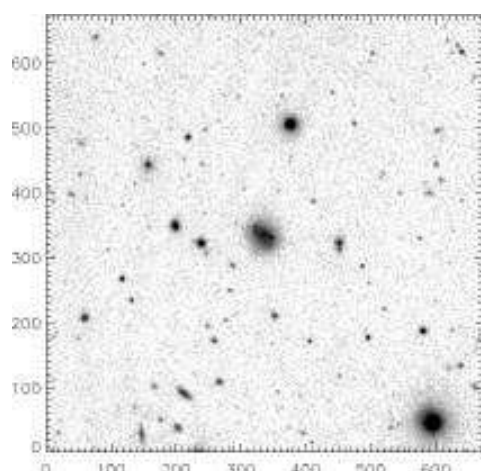


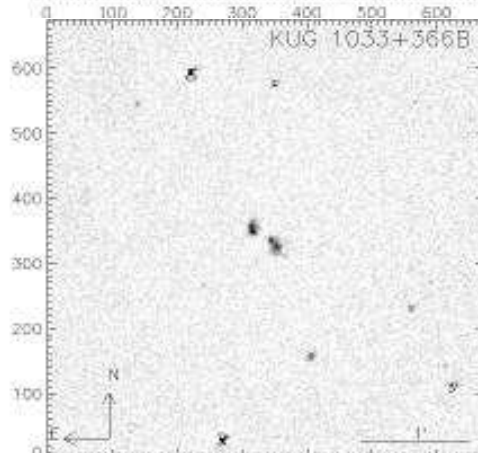
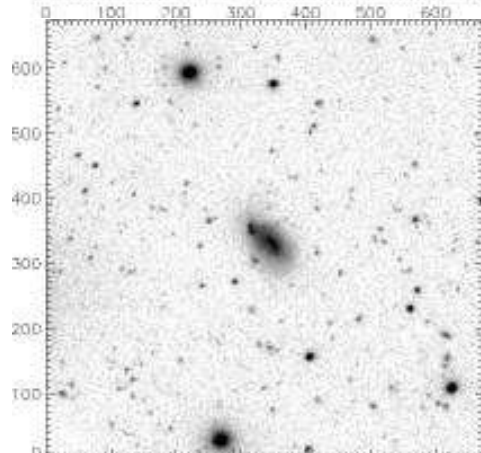
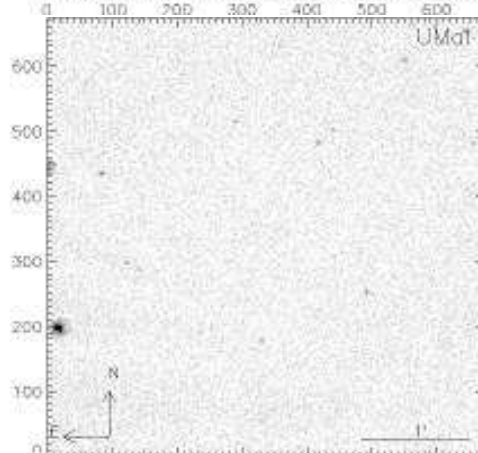
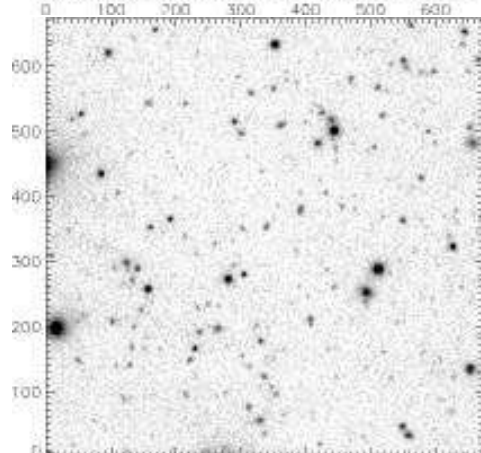
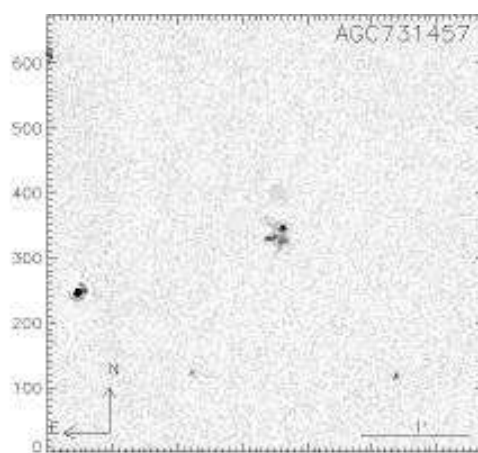
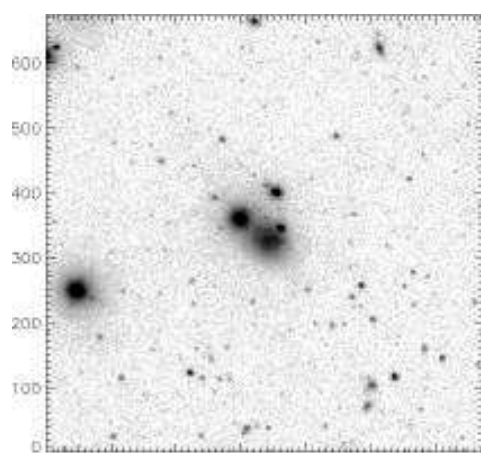


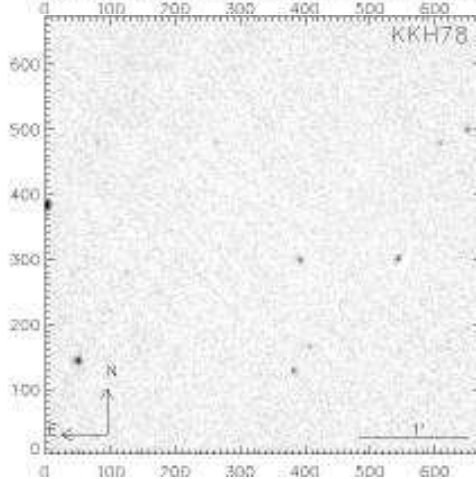
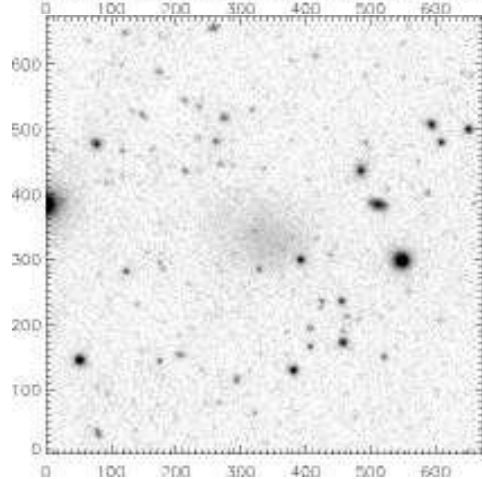
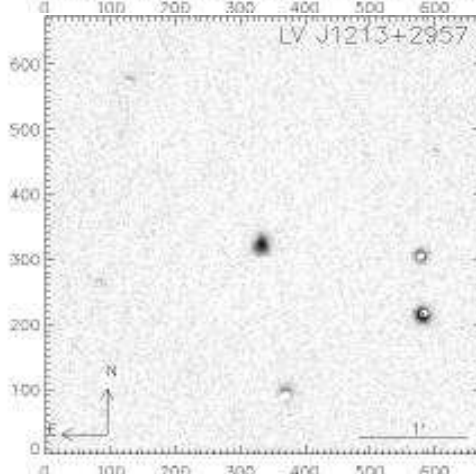
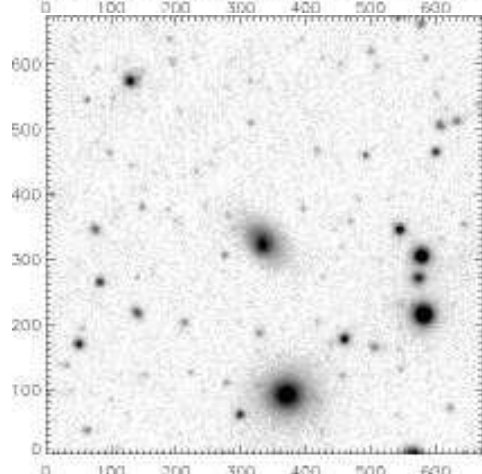
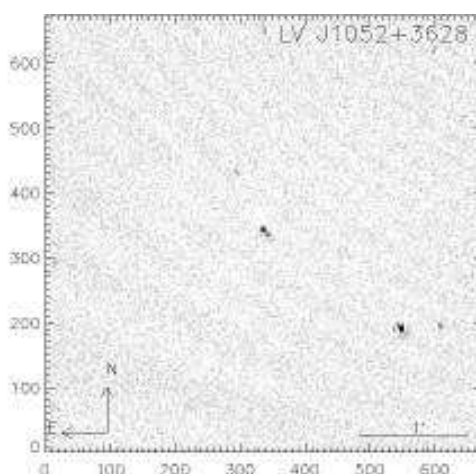
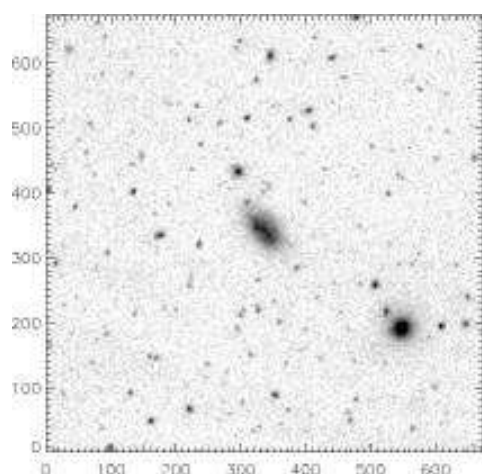


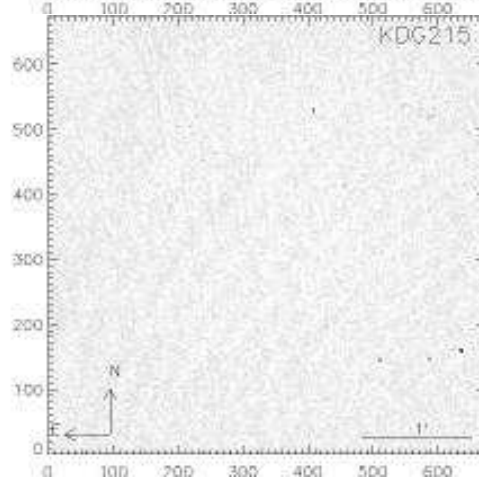
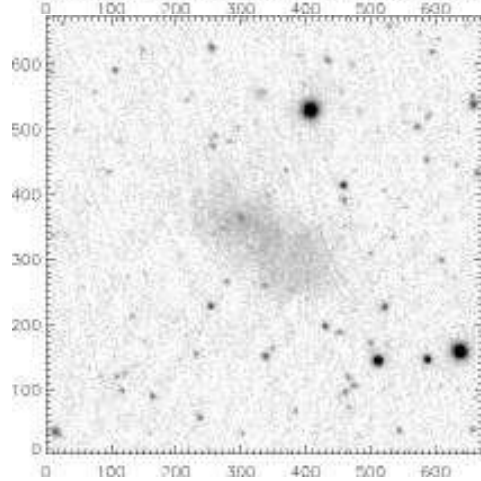
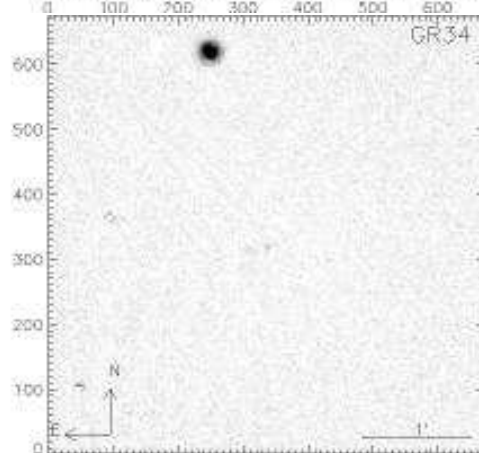
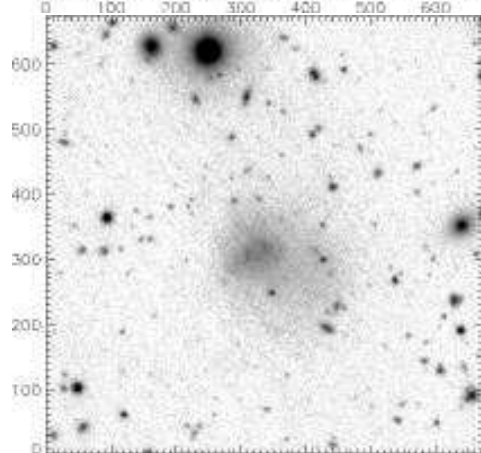
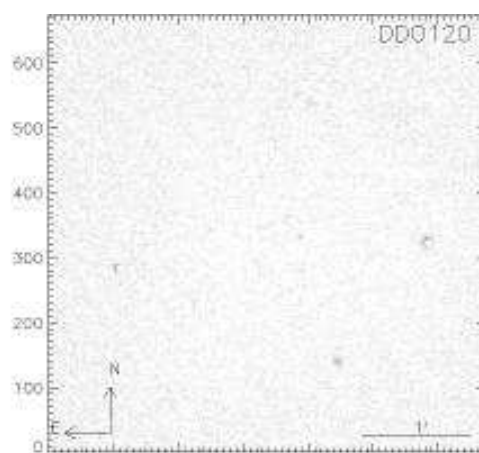
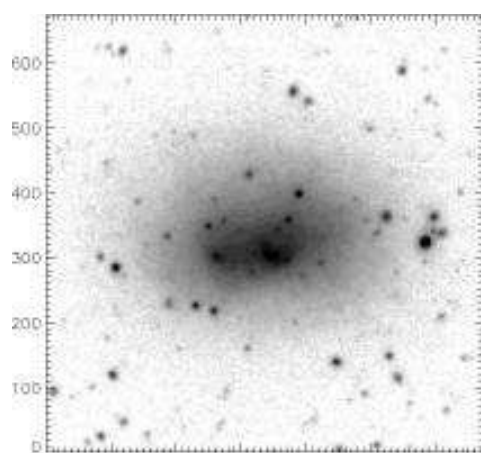


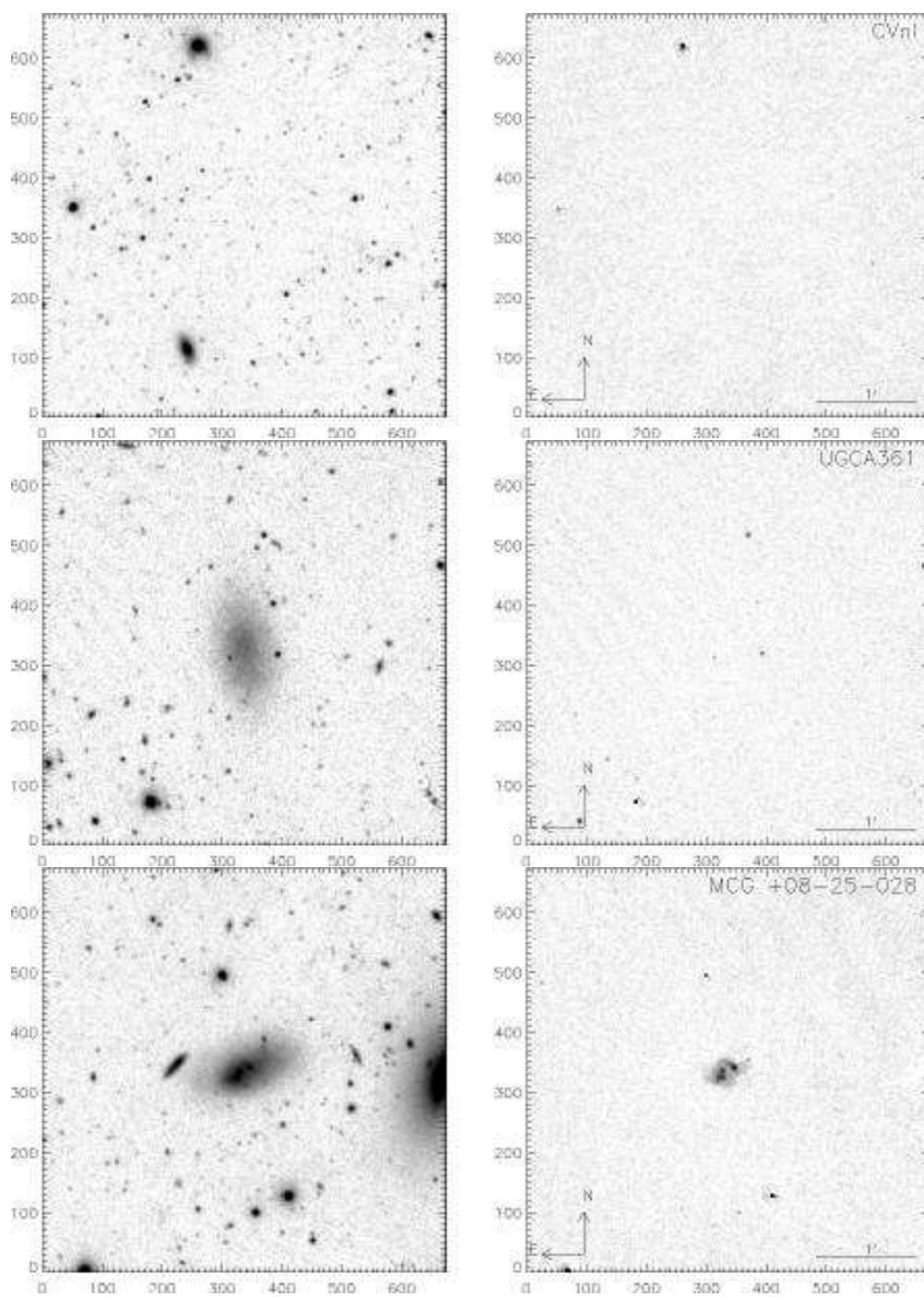


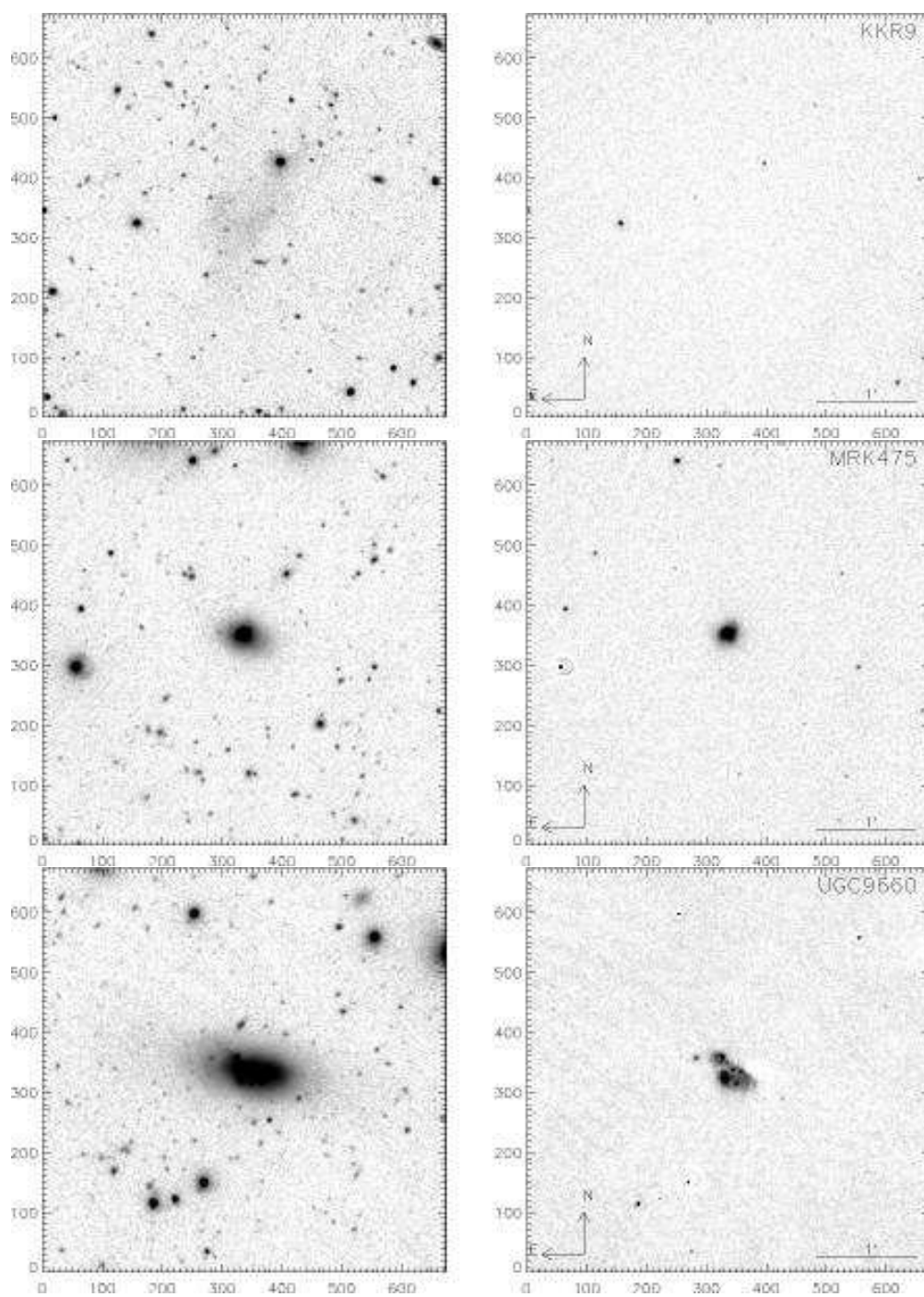


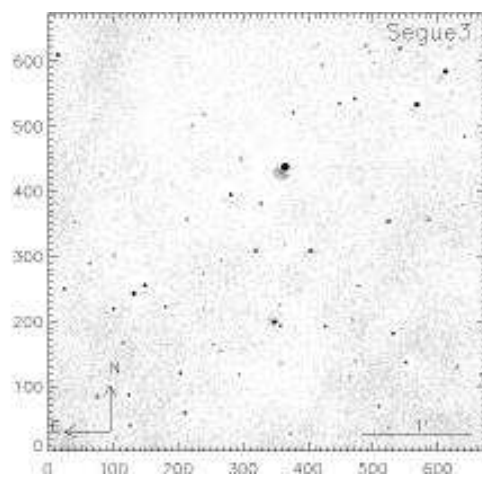
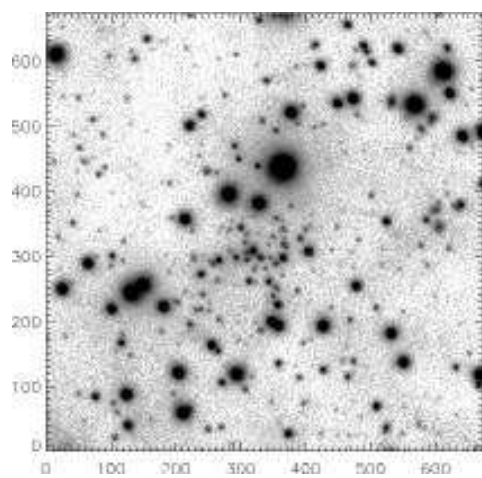
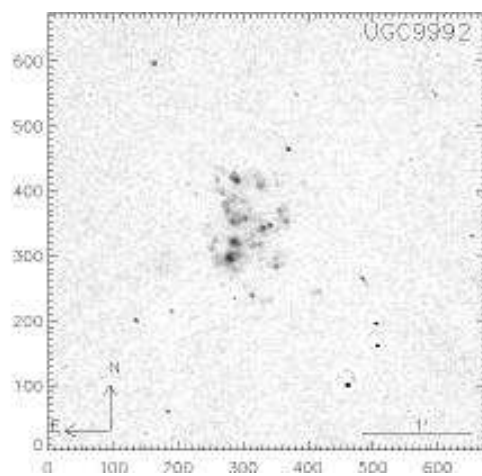
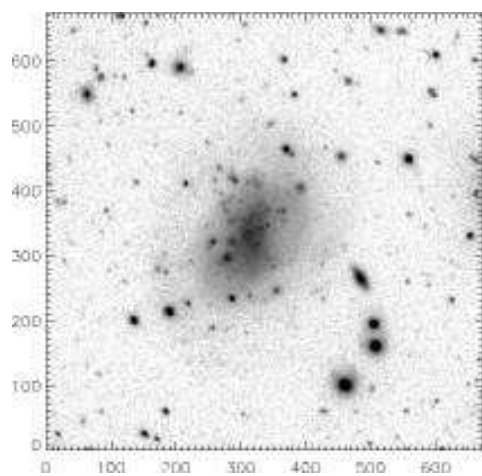


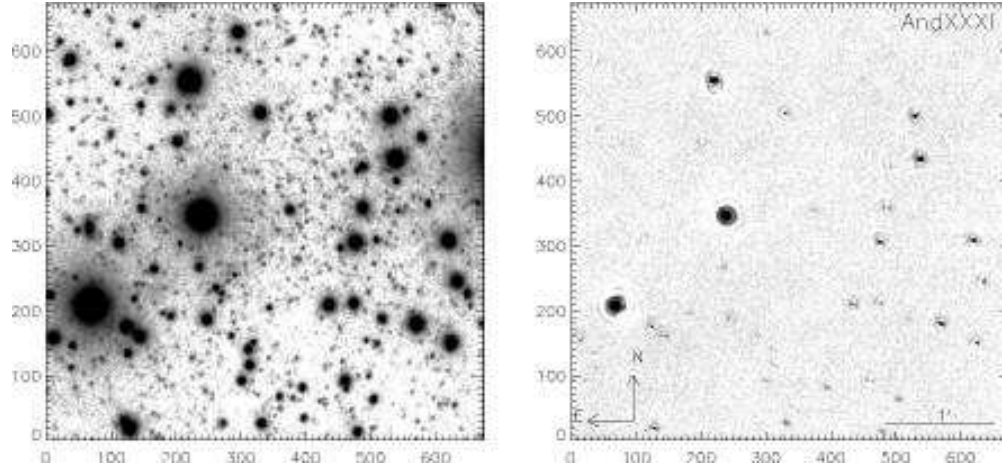












-
1. I. D. Karachentsev, S. S. Kaisin, Z. Tsvetanov, and H. Ford, *Astronom. and Astrophys.***434**, 935 (2005).
 2. S. S. Kaisin and I. D. Karachentsev, *Astrophysics* **49**,287 (2006).
 3. I. D. Karachentsev and S. S. Kaisin, *Astronom. J.***133**, 1883 (2007).
 4. S. S. Kaisin and I. D. Karachentsev, *Astronom. and Astrophys.***479**, 603 (2008).
 5. I. D. Karachentsev and S. S. Kaisin, *Astronom. J.***140**, 1241 (2010).
 6. S. S. Kaisin, I. D. Karachentsev, and E. I. Kaisina, *Astrophysics* **54**, 315 (2011).
 7. S. S. Kaisin and I. D. Karachentsev, *Astrophysics* **56**, 305 (2013).
 8. S. S. Kaisin and I. D. Karachentsev, *Astrophysical Bulletin***68**, 381 (2013).
 9. I. D. Karachentsev, D. I. Makarov, and E. I. Kaisina, *Astronom. J.***145**, 101 (2013).
 10. E. I. Kaisina, D. I. Makarov, I. D. Karachentsev, and S. S. Kaisin, *Astrophysical Bulletin***67**, 115, (2012).
 11. V. L. Afanasiev and A. V. Moiseev, *Astronomy Lettets* **31**, 194 (2005).
 12. J. B. Oke, *Astronom. J.***99**, 1621 (1990).
 13. R. C. Kennicutt, *Annu. Rev. Astronom. Astrophys.***36**, 189 (1998).
 14. D. J. Schlegel, D. P. Finkbeiner, and M. Davis, *Astrophys. J.* **500**, 525 (1998).
 15. M. A. W. Verheijen, *Astrophys. J.* **563**, 694 (2001).
 16. J. C. Lee, R. C. Kennicutt, J. G. Funes, et al., *Astrophys. J.* **692**, 1305 (2009).
 17. A. Gil de Paz, S. Boissier, B. F. Madore, et al., 2007, *Astrophys. J. Suppl.***173**, 185 (2007).
 18. N. F. Martin, C. T. Slater, E. F. Schlafly, et al., *Astrophys. J.* **772**, 15 (2013).
 19. N. F. Martin, E. F. Schlafly, C. T. Slater, et al.,

- Astrophys. J. **779L**, 10 (2013).
20. A. D. Mackey, A. P. Huxor, N. F. Martin, et al., *Astrophys. J.* **770L**, 17 (2013).
 21. D. Martinez-Delgado, J. Fliri, R. Laesker, et al. (in preparation).
 22. V. Belokurov, M. G. Walker, N. W. Evans, et al., *Monthly Notices Roy. Astronom. Soc.* **397**, 1748 (2009).
 23. B. Willman, J. J. Dalcanton, D. Martinez-Delgado, et al., *Astrophys. J.* **626L**, 85 (2005).
 24. D. B. Zucker, V. Belokurov, N. W. Evans, et al., *Astrophys. J.* **643L**, 103 (2006).
 25. V. Belokurov, M. G. Walker, N. W. Evans, et al., *Astrophys. J.* **712L**, 103 (2010).
 26. J. B. Jensen, J. L. Tonry, B. J. Barris, et al., *Astrophys. J.* **583**, 712 (2003).
 27. B. S. Koribalski, L. Staveley-Smith, V. Kilborn, et al., *Astronom. J.* **128**, 16 (2004).
 28. E. Bernstein-Cooper, J. M. Cannon, and E. A. Adams, *Astronom. J.* **148**, 35 (2014).
 29. K. N. Abazajian, J. K. Adelman-McCarthy, M. A. Agüeros, et al. *Astrophys. J. Suppl.* **182**, 543 (2009).
 30. I. D. Karachentsev, O. G. Nasonova, and H. M. Courtois, *Astrophys. J.* **743**, 123 (2011).
 31. I. D. Karachentsev, R. B. Tully, P. F. Wu, et al., *Astronom. J.* **782**, 4 (2014).
 32. R. B. Tully and J. R. Fisher, 1977, *Astronom. and Astrophys.* **54**, 661 (1977).
 33. J. Pflamm-Altenburg, C. Weidner, and P. Kroupa, *Astrophys. J.* **671**, 1550 (2007).
 34. I. D. Karachentsev and E. I. Kaisina, *Astronom. J.* **146**, 46 (2013).
 35. I. D. Karachentsev, V. E. Karachentseva, O. V. Melnyk, and H. M. Courtois, *Astrophysical Bulletin* **68**, 243 (2013).